International Journal of Rotating Machinery
2001, Vol. 7, No. 4, pp. 271–284
Reprints available directly from the publisher
Photocopying permitted by license only

Flow Field in the Turbine Rotor Passage in an Automotive Torque Converter Based on the High Frequency Response Rotating Five-hole Probe Measurement

Part II: Flow Field at the Off-design Condition and Effects of Speed Ratio

Y. F. LIU*, B. LAKSHMINARAYANA† and J. BURNINGHAM

Center for Gas Turbines and Power, The Pennsylvania State University, University Park, PA 16802

(Received 11 May 2000; In final form 23 May 2000)

The flow field at the design condition was presented and interpreted in Part I. The flow field at one off-design condition (Speed Ratio 0.065) is presented and interpreted in this part. In addition, the hydraulic performance is analyzed by using flow measurement results both upstream and downstream of the turbine and inside the turbine rotor passage. It is found that at the off-design conditions, especially the near stall condition (Speed Ratio 0.065), most of the pressure drop occurs in the first half of turbine passage. About 82% of the total torque is extracted between the turbine inlet and the middle plane. In addition, the shell develops torque at nearly five times the rate of core. Furthermore, the higher the speed ratio, the higher the total pressure drop. Loss is maximum at the near stall condition and varies almost linearly with the speed ratios. A compromise has to be made between the design and the off-design performance in order to improve the overall performance and fuel economy of torque converters.

Keywords: Torque converter; Turbine; Flow field; Off-design condition; Speed ratio effect

INTRODUCTION

Turbomachinary design usually is an iterative process involving a trade-off between the aerodynamic performance at the design and off-design conditions. A torque converter is widely used in today's automatic transmission of vehicles. Its hydraulic performance has a significant

*Tel.: 814 863-0156, Fax: 814 865-7092, e-mail: yxl163@psu.edu
†Corresponding author. Tel.: 814 865-5551, Fax: 814 865-7092, e-mail: bllaer@engr.psu.edu

influence on vehicle fuel economy and power performance.

The torque converter, especially the turbine, however, operates in a wide range of operating conditions. Consequently, the inlet flow angle will vary from the design values, which leads to additional losses. These are commonly referred to as off-design losses. The off-design conditions have a major impact on the performance of the torque converter. In addition, these flows can affect the durability of the torque converter.

In order to improve the performance and fuel economy of the automotive torque converter, an understanding of the off-design flow field is also important. The flow field at the design condition ($SR = 0.6$) is presented in the first part of this paper: Liu and Lakshminarayana (2000), "Flow Field in the Turbine Rotor Passage in an Automotive Torque Converter based on the High Frequency Response Rotating Five-Hole Probe Measurement", Part I: Flow Field at the Design Condition (Speed Ratio 0.6)", In this part of the paper, the flow field at the off-design condition ($SR = 0.065$) is presented and interpreted. In addition, the effects of speed ratio on the performance of the torque converter are also discussed.

Experimental Facility and Programs

The torque converter research facility, the rotating five-hole probe traverse mechanism, and the instrumentation used in this investigation are described in detail in the first part of this paper. Furthermore, all the normalization procedures and performance parameter definitions are the same as described in Part 1. This experiment is carried out at the near stall condition ($SR = 0.065$), with the pump rotating speed 800 rpm and the turbine rotating speed 52 rpm.

The definition used to determine the blade-to-blade averaged torque is given below:

$$\tau = \int U_1 V_{\theta_1} \rho V_{z_1} dA_1 - \int U_2 V_{\theta_2} \rho V_{z_2} dA_2 \qquad (1)$$

where U is the blade speed, V is the absolute velocity, ρ and A is the density and the area of the cross section respectively.

RESULT AND DISCUSSIONS

Some typical data are presented and interpreted in this paper. Reader is referred to Liu (2001); Burningham (1997) for comprehensive data. At the near stall condition ($SR = 0.065$), the turbine rotational speed is very small (52 rpm), so the rotational effect is negligible and the dominant effects are the curvature and flow turning. In general, the flow pattern within the turbine passage is influenced by many factors, that is, the inlet velocity and pressure distribution, the inlet flow angle, the rotating speed, the geometry of the blade, and so on. Concerning the effect of rotation, the rotation number is introduced (Lakshminarayana, 1996, p. 390):

$$R_o = \frac{\text{Coriolis\_Force}}{\text{Inertia\_Force}} = \frac{\Omega L}{W}$$

where Ω is the angular speed of the rotor, L is a characteristic length, and W is a characteristic velocity. The rotation number is the ratio of the Coriolis force (ΩW) to the inertial force (W^2/L) and is a measure of the importance of rotation on the flow field. For centrifugal machinery, appropriate variables for L is chord length, and the characteristic velocity is the total free-stream relative velocity. The mass flow rate didn't change much from the design condition ($SR = 0.6$) to the near stall condition ($SR = 0.065$). The measured volumetric flow rate at the design condition ($SR = 0.6$) is $0.028\,m^3/s$. While at the near stall condition ($SR = 0.065$), the volumetric flow rate is $0.032\,m^3/s$ (Marathe, 1998). Thus, the through flow velocity didn't change much with the speed ratios. The dominant term in the Rotation number is the angular speed of the rotor. Since the rotational speed at speed ratio 0.6 (696 rpm) is much higher than that at speed ratio 0.065 (52 rpm), the rotation number at speed ratio 0.6 is much bigger than that at the speed ratio 0.065

(about 15 times). Consequently it can be concluded that the rotation effect is insignificant at the near stall condition ($SR = 0.065$). The centrifugal force due to the passage curvature in the meridional plane has the dominant influence at this speed ratio. Another important factor that affects the flow field is the centrifugal force by blade curvature on blade-to-blade surface.

Static Pressure *P* Field

The contour plots of static pressure at the turbine 1/4 chord, turbine mid-chord, and turbine 4/4 chord are shown in Figures 1a–c respectively. According to the basic theory of turbomachinery, there are three sources that contribute to the static pressure drop along a streamline. The first source is the centrifugal force. The second source is the static pressure drop due to acceleration of the relative velocity. The third source is the pressure loss due to viscous effects. At the near stall condition ($SR = 0.065$), the static pressure drop due to centrifugal force can be negligible, as the turbine is almost stationary. Thus most of the static pressure drop is attributed to the acceleration of the relative total velocity and the viscous loss. From the turbine 1/4 chord to the turbine mid-chord, the flow experiences pressure rise rather than pressure drop near the shell region. Since viscous effect always causes static pressure drop, the only explanation to this phenomenon is that the flow decelerates from the turbine 1/4 chord to the turbine mid-chord. Due to the "jet-wake" flow pattern inside the pump rotor passage, the turbine receives high pressure and velocity fluid from the upstream pump rotor near the shell region. At the turbine mid-chord, the distribution is conventional with low pressure near the suction side and high pressure near the pressure surface.

Furthermore, there is some static pressure rise from the turbine 1/4 chord to the turbine mid-chord in other regions besides the shell in the turbine rotor passage. At this speed ratio, there is a large positive incidence angle at the turbine leading edge; this may result in high incidence losses. In addition, the pressure drop at this speed ratio is mainly caused by the intense mixing near the leading edge and viscous effect along the turbine passage. Due to both the high incidence and the high viscous losses, the static pressure at the

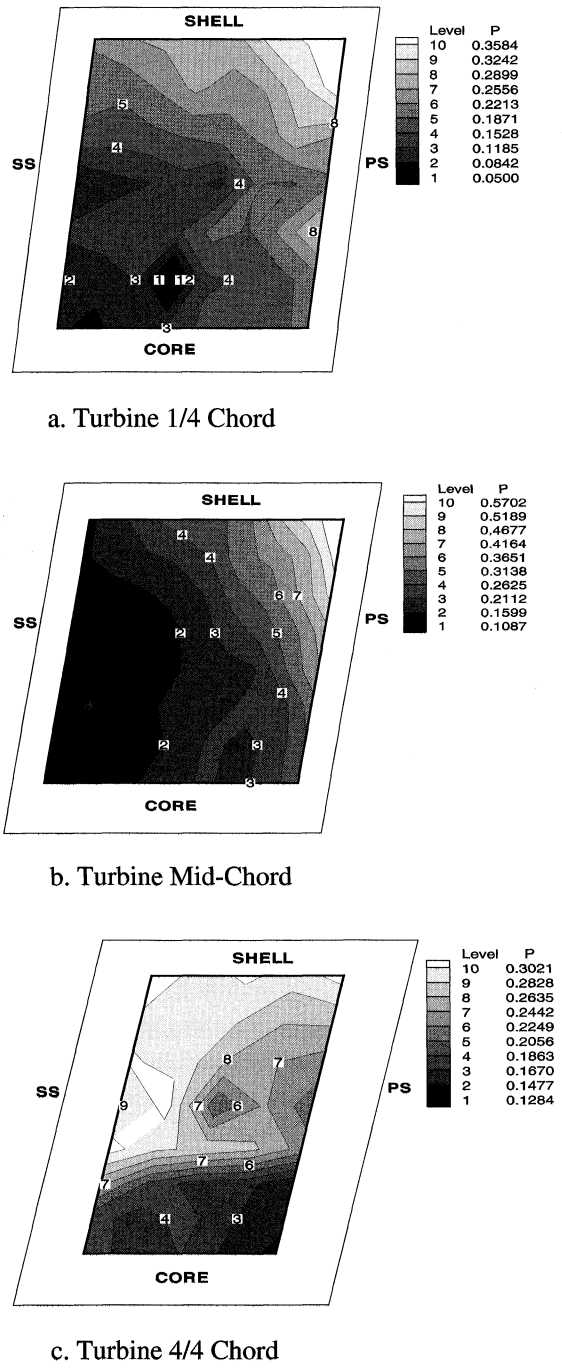

FIGURE 1 Contour plots of static pressure P ($SR = 0.065$).

turbine 1/4 chord is even lower than that at the turbine mid-chord in some regions at this speed ratio.

Absolute Stagnation Pressure $(P_0)_a$ Field

Figures 2a–c show the contour plots of the absolute stagnation pressure at the turbine 1/4 chord, mid-chord, and turbine 4/4 chord respectively. The general pressure field trends at the near stall condition ($SR = 0.065$) are similar to those observed at the design condition ($SR = 0.6$). At this speed ratio, the contour plots show less significant variation both in the radial direction and in the tangential direction compare to the design condition ($SR = 0.6$). Both the lower rotational speed and the associated flow turning effect contributes to less significant variation in the radial direction and the tangential direction compared with the design condition ($SR = 0.6$).

In addition, it can be seen that the static pressure distribution (Fig. 1) at the turbine 1/4 chord is relatively more uniform tangentially than the distribution of the absolute stagnation pressure (Fig. 2). The low absolute stagnation pressure near the core/suction side corner can be attributed to the low relative total velocity at this region. Because the turbine is almost stationary at this speed ratio, both the relative and absolute velocities are low. As a result, the absolute stagnation pressure exhibits pronounced variations, which is different from the static pressure distribution. At the turbine mid-chord and the turbine 4/4 chord, the distribution of absolute stagnation pressure has the same trend as the static pressure.

Finally, there is a slight pressure increase from the turbine mid-chord to the turbine 4/4 chord near the core region. The absolute stagnation pressure is the sum of static pressure and the absolute dynamic pressure. There is a large incidence angle at the turbine leading edge at this speed ratio, and this results in a large separation area in the first half of the turbine passage at the core/suction side corner. On the other hand, the meridional curvature effect begins to dominate and flow accelerates in the second half of the turbine passage. Since the flow separation is eliminated, the related intense mixing vanishes. Thus the absolute stagnation pressure increases a little bit in the second half of the turbine passage.

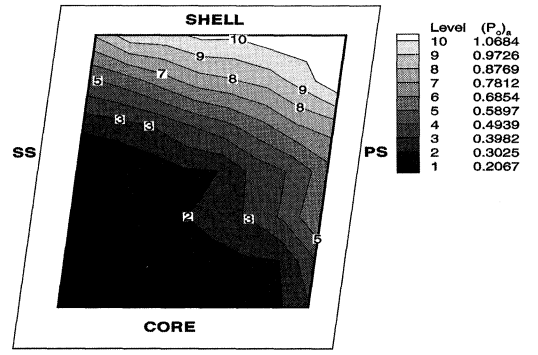

a. Turbine 1/4 Chord

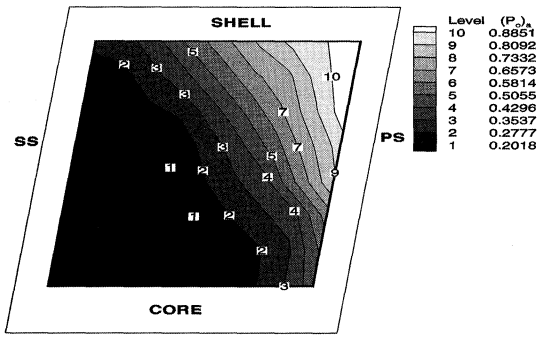

b. Turbine Mid-Chord

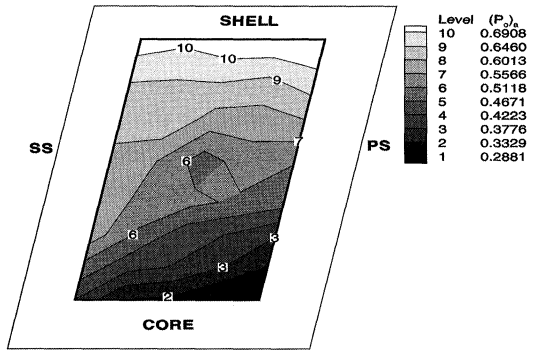

c. Turbine 4/4 Chord

FIGURE 2 Contour plots of absolute stagnation pressure $(P_0)_a$ ($SR = 0.065$).

Mass Averaged Absolute Stagnation Pressure Drop $(P_{0a})_m$

The mass averaged absolute stagnation pressure drop from the turbine inlet to the turbine exit at the near stall condition ($SR = 0.065$) is shown in Figure 3a. It can be clearly seen that most of the pressure drop takes place in the first half of the turbine passage, especially in the first quarter of the turbine passage. This is mainly due to the high incidence angle at this speed ratio and the associated large area of flow separation.

Furthermore, there is a slight pressure rise from the turbine mid-chord to the turbine 4/4 chord (turbine trailing edge location), which is mainly due to flow reattachment. Since the centrifugal force is insignificant at this speed ratio, the static pressure drop is small; thus the dynamic head is the dominant term. This may indicate that the flow separates at the leading edge and is not able to reattach till after the turbine mid-chord. In addition, there is a higher mixing loss downstream of the turbine trailing edge due to intense mixing between the wake and the free stream fluid at this off-design condition.

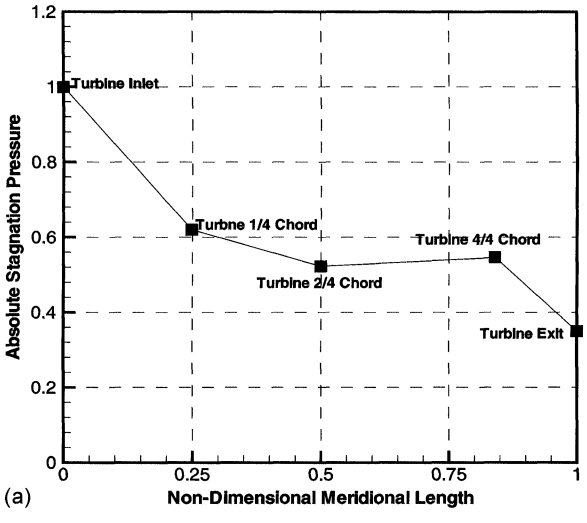

FIGURE 3 Absolute stagnation pressure distribution ($SR = 0.065$). (a) Mass averaged absolute stagnation pressure $(P_{oa})_m$ drop ($SR = 0.065$); (b) Radial distribution of blade-to-blade averaged absolute stagnation pressure $(P_{oa})_b$ ($SR = 0.065$).

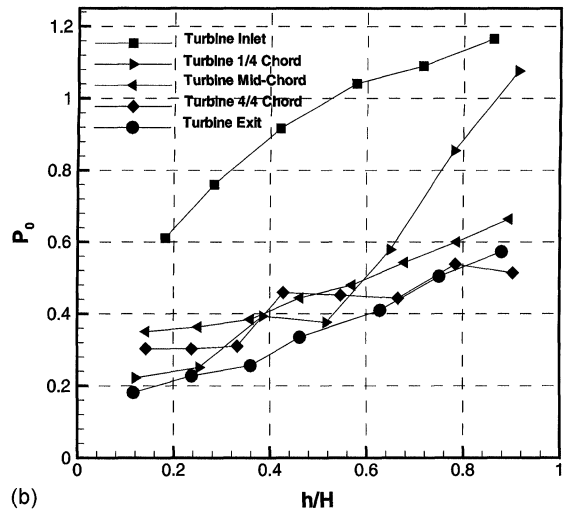

FIGURE 3 (Continued).

Radial Distribution of Blade-to-blade Averaged Absolute Stagnation Pressure $(P_{0a})_b$

The radial distribution of blade-to-blade averaged absolute stagnation pressure, $(P_{0a})_b$, is shown in Figure 3b for speed ratio 0.065. It can be seen that the pressure drop in the first half of the turbine is much larger than in the second half. The ratio of the pressure drop between the two halves is much greater at this speed ratio than at the design speed ratio. One explanation for this is that there is a large incidence angle at the leading edge of the turbine blades. This would cause the first half of the blade passage to do a majority of the flow turning, and therefore there would be a greater pressure drop. Another contributor is the larger separation region seen in the suction side/core corner at the turbine 1/4 chord and mid-chord measurement planes. Thus there would be an additional pressure drop due to a high level of viscous dissipation in the first half of the turbine.

Furthermore, the pressure drop is larger near the shell than near the core region, which is similar to that observed at the design condition ($SR = 0.6$). This phenomenon is attributed to the upstream pump exit flow field. The turbine receives much higher pressure fluid at the shell than at the core from the upstream pump rotor at this speed

ratio, as was seen at speed ratio 0.6. This is caused by nearly separated flow near the core, which gives rise to lower pressure rise across the pump. The pressure drop near the core is low for the first half of the turbine. It is likely that there is low work output in this region, and thus the pressure drop may be mostly due to viscous dissipation associated with the suction side/core corner separation. In the second half of the turbine, there is a greater pressure drop near the core than at the shell. Since it is unlikely that there is a higher work output near the core, this pressure drop must then be simply a continuation of the high viscous losses occurring near the core. Still, the pressure drop is overall much lower in the second half of the turbine. Thus, a lower work output is to be expected from the fluid in the second half of the turbine.

Relative Total Velocity $(W_o)_t$ Field

The contour plots of the relative total velocity at the turbine 1/4 chord, mid-chord, and turbine 4/4 chord at the near stall condition ($SR = 0.065$) are shown in Figures 4a – c respectively. It can be seen that at the turbine 1/4 chord where the flow has just been turned radially from an axial direction, the relative total velocity is higher in the shell/pressure side corner and much lower at the core/suction side corner. In addition, the tangential velocity gradient is less significant than the velocity variation in the radial direction. The radial pressure gradient is mainly caused by the meridional curvature, while the tangential pressure gradient arises due to both the flow turning and the Coriolis force. At this speed ratio, the Coriolis force is negligible due to the very low turbine rotational speed. Thus, the tangential pressure gradient is not as significant as that observed at the design condition ($SR = 0.6$).

Furthermore, high momentum regions are observed near shell/pressure side corner, and low momentum regions are located near core/suction corner at the turbine 1/4 chord and the turbine mid-chord. From the turbine 1/4 chord to the turbine mid-chord, the low velocity region expands; and this is attributed to the rapid change of flow direction in both the meridional direction and along the camber line. At the turbine 4/4 chord,

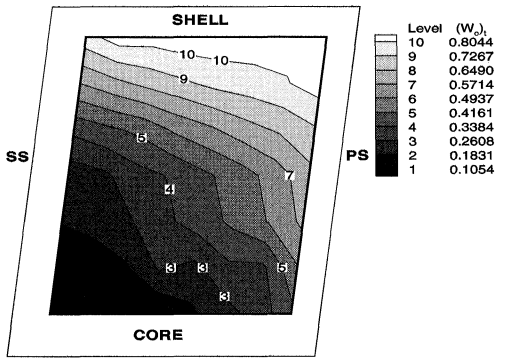

a. Turbine 1/4 Chord

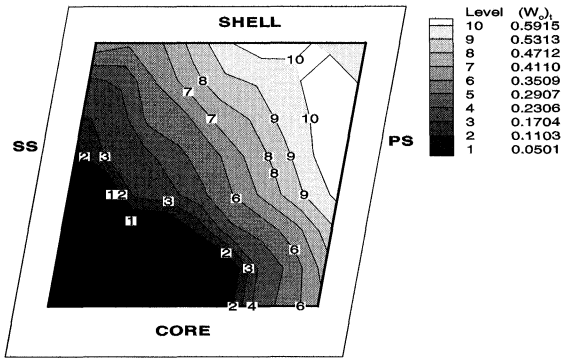

b. Turbine Mid-Chord

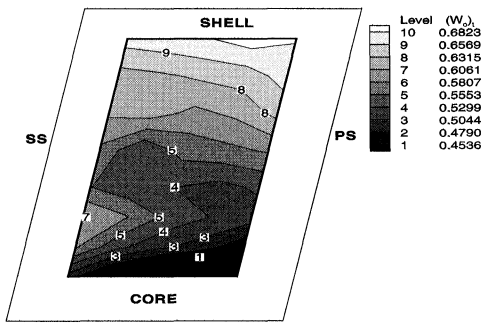

c. Turbine 4/4 Chord

FIGURE 4 Contour plots of relative total velocity $(W_o)_t$ ($SR = 0.065$).

the high momentum fluid is located near the shell/pressure side corner, which is the same as the turbine 1/4 chord and the turbine mid-chord. The low momentum fluid, however, is located near the core/pressure side corner. The migration of this low momentum fluid can be attributed to the secondary flow, which arises from the non-uniform inlet flow and high flow turning. The low momentum fluid, which is concentrated near the core/suction side corner up to the mid-chord, is mainly due to the combined effect of "jet-wake" flow pattern at the pump exit and the large incidence angle at the turbine leading edge.

The low velocity region at the turbine 2/4 chord is located near the core/suction side corner at this speed ratio rather than near the middle of the suction side as observed at speed ratio 0.6. This difference can be attributed to the effect of Coriolis force. At the design condition ($SR = 0.6$, 696 rpm), the turbine rotational speed is much higher than at the near stall condition ($SR = 0.065$, 52 rpm). Thus the Coriolis force caused by the turbine rotation is much stronger, and it is this Coriolis force that has a significant effect on the velocity distribution in the blade-to-blade direction. In addition, the Coriolis force is at the peak at the turbine mid-chord, since the flow path is at the radial direction at this measurement plane. Because of the flow path orientation and the high rotational speed, the low momentum fluid concentrates near the middle of the suction side at the design condition ($SR = 0.6$), and the low momentum fluid is located near the core/suction side corner at the near stall condition ($SR = 0.065$). The Coriolis force is much weaker at the turbine 1/4 chord and the turbine 4/4 chord, since the flow is turned from the axial/radial direction to radial/axial direction respectively. Therefore, the relative velocity has similar distribution between these two speed ratios.

The radial distribution of blade-to-blade averaged relative total velocity, $(W_{ot})_b$, for the near stall condition ($SR = 0.065$) are given in Figure 5. As was seen at the design condition ($SR = 0.6$), the inlet total velocity is significantly higher than

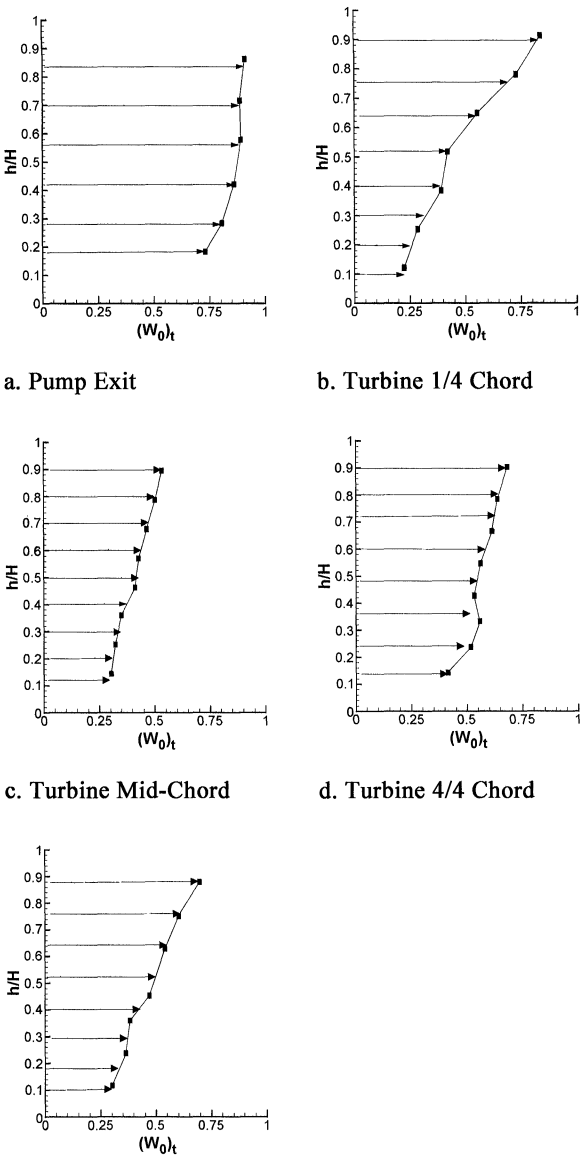

FIGURE 5 Radial distribution of blade-to-blade averaged relative total velocity $(W_{ot})_b$ ($SR = 0.065$).

those observed at other four measurement planes at the near stall condition ($SR = 0.065$). Because the inlet measurements were taken in the gap between the two rotors, the flow has not entered the turbine blade ducts. Thus, there is still a high tangential velocity component present, which was produced by the pump. At the turbine 1/4 chord

and the turbine mid-chord, the flow is highly non-uniform due to large area of flow separation. In addition, since the through flow velocity is greater at low speed ratios, the radial velocity gradient would also be larger at this speed ratio ($SR = 0.065$) than at the design condition ($SR = 0.6$). The velocity is more uniform at the turbine inlet and 4/4 chord than the velocity distribution at the turbine 1/4 and mid-chord. As mentioned before, the centrifugal force due to rotation is negligible at the near stall condition, and the dominant factor is the centrifugal force due to streamline curvature. The evolving flow in the streamwise direction is subjected to strong centrifugal force, thus causing the bulk of the flow to move toward the outer radius, that is, the shell region. This can be seen clearly in Figures 5b and c as the velocity deficit near the core region at the turbine 1/4 and mid-chord. From the turbine mid-chord to the turbine 4/4 chord, the large positive incidence effect diminishes and the convex curvature begins to dominate, thus the separated flow begin to reattach, and the velocity becomes more uniform near the turbine trailing edge location.

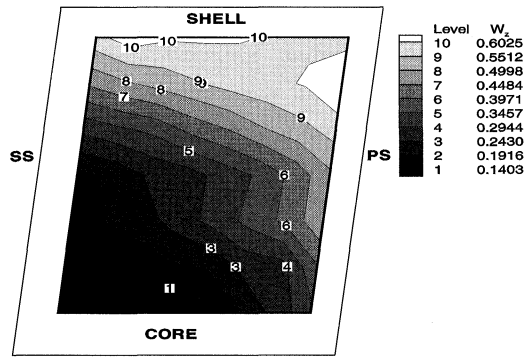

a. Turbine 1/4 Chord

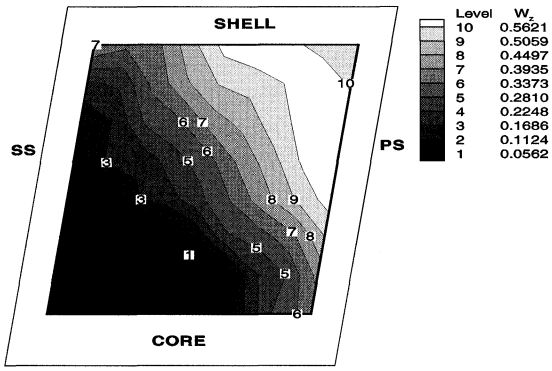

b. Turbine Mid-Chord

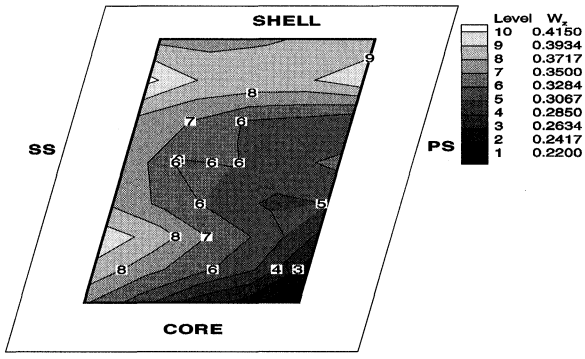

c. Turbine 4/4 Chord

FIGURE 6 Contour plots of through flow velocity (W_z) ($SR = 0.065$).

Through Flow Velocity W_z Field

The contour plots of through flow velocity at the turbine 1/4 chord, mid-chord, and turbine 4/4 chord at the near stall condition ($SR = 0.065$) are shown in Figures 6a–c, respectively. A strong "jet-wake" flow structure can be clearly seen at the turbine 1/4 chord and turbine mid-chord. The "jet" flow is located near the shell/pressure side corner, and the low velocity "wake" flow concentrates near the core/suction side corner. This "jet-wake" flow structure may be attributed to the upstream pump exit flow and the large positive incidence angle at this speed ratio. Due to the flow separation, the effective through flow area is significantly reduced, and this blockage effect enhances the "jet-wake" flow pattern at the turbine 1/4 chord and the turbine mid-chord. On the other hand, the flow is relatively uniform at the turbine 4/4 chord, which implies that the flow is able to reattach before the turbine trailing edge.

In addition, the flow separation area increases from the turbine 1/4 chord to the turbine mid-chord. At the turbine 1/4 chord, the separation area is about 15% of the passage area, while it is about 35% of the passage area at the turbine 2/4 chord. The cause of this increased separation area is the high incidence flow into the turbine inlet. The flow stalls and separates at the turbine leading edge of the turbine blades, the adverse pressure gradient that exists from the turbine 1/4 chord to the mid-chord (Fig. 1) is also responsible for this flow separation and its expansion.

Flow Yaw Angle β_t Field

The contour plots of flow yaw angle at the speed ratio 0.065 are shown in Figure 7. It should be mentioned that the turbine inlet flow was measured in the gap between the pump trailing edge and the turbine leading edge. Thus some variation is expected between the flow field at the turbine leading edge and the inlet flow shown here. The turbine inlet angle is 61.4°, and it can be seen that the turbine encounters large positive incidence from the upstream pump. This large positive incidence angle results in high relative velocity and high blade loading near the turbine leading edge. The negative incidence is about $-30°$, and it is only found near the core region. There are large variations in the incidence from the core to the shell. However, the distribution in the tangential direction is relatively uniform. At the turbine 1/4 chord, the blade angle is 48.1° at this measurement plane, and all the flow in the turbine passage is overturned. The distribution of relative yaw angle at this measurement plane is nearly uniform from the core to the shell in most of the passage except the middle of the core region. The flow in this region is substantially overturned. This is consistent with the low through flow velocity observed in this region.

The blade angle is nearly 0° at the turbine mid-chord. The flow near the shell region is underturned, and those near the core region are overturned. At the turbine mid-chord, there is a

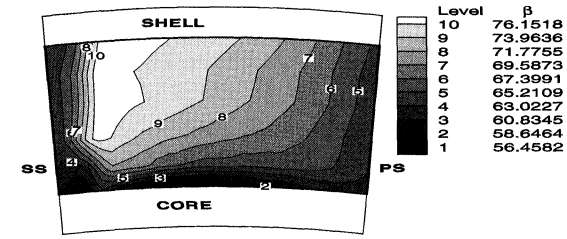

a. Turbine Inlet

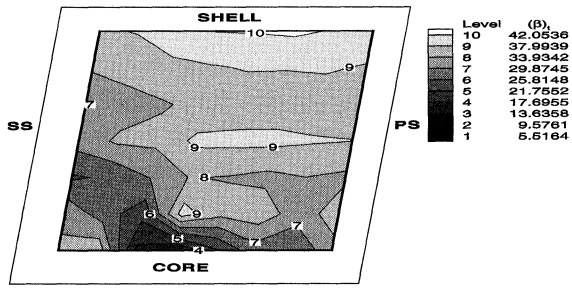

b. Turbine 1/4 Chord

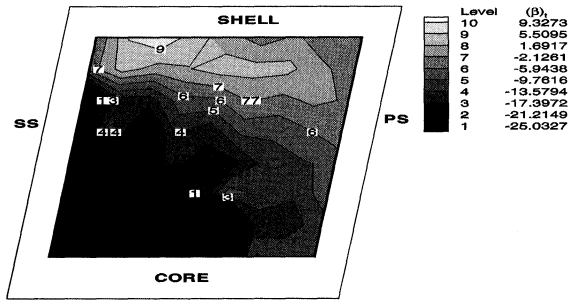

c. Turbine Mid-Chord

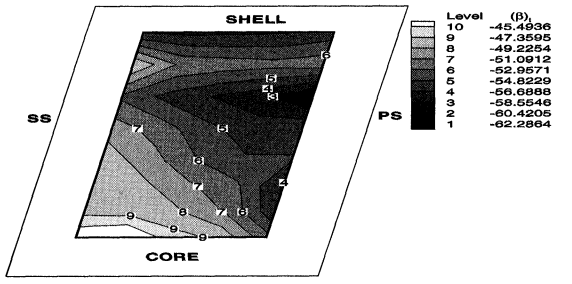

d. Turbine 4/4 Chord

FIGURE 7 Contour plots of relative flow yaw angle (β_t) ($SR = 0.065$).

blank region at the core/suction side corner. At this region, the flow is nearly separated, and the relative flow yaw angle is beyond the calibration range of the five-hole probe used in the test. The yaw angle shows a large variation both from the core to the shell and from the suction surface to the pressure surface at this measurement plane. It varies from $-25°$ near the core/suction side corner to 9.32° at the pressure side/shell corner. Thus the flow field is highly three dimensional at the turbine mid-chord.

At the turbine 4/4 chord, the blade angle is $-58.47°$. Most of the flow at the turbine 4/4 chord is underturned. The flow is much more uniform than those at the turbine 1/4 chord and the turbine mid-chord, and the maximum deviation angle is around 10° near the core region. The deviation angle is related to the passage width, the flow path, and the blade number. Since the flow path in the core region is much shorter than that near the mid-span and the shell region, the deviation should be relatively higher there.

Rotary Stagnation Pressure P^* Field

The contour plots of rotary stagnation pressure (Defined in Part I, Eq. (4)) is shown in Figure 8. The rotary stagnation pressure along a streamline should remain constant in inviscid flow. The difference in rotary stagnation pressure between two locations represents the viscous losses. Based on this, the viscous losses from the turbine inlet to the turbine mid-chord plane is much higher than the viscous losses in the second half of the turbine passage. This confirms that there exists large incidence losses at this speed ratio and intense mixing losses due to flow separation in the first half of the turbine passage. It is expected that the efficiency in the second half should be much higher than that in the first half.

Blade-to-blade Averaged Flow Properties and Turbine Torque

The radial distributions of blade-to-blade averaged relative total pressure, $(P_{or})_b$, from the pump

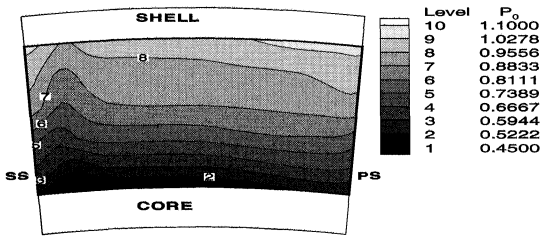

a. Turbine Inlet

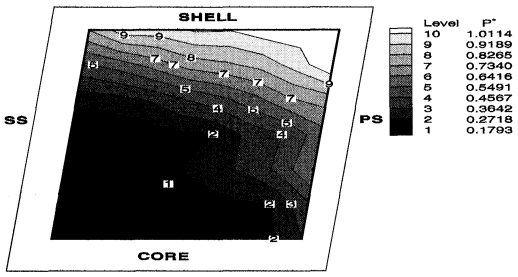

b. Turbine 1/4 Chord

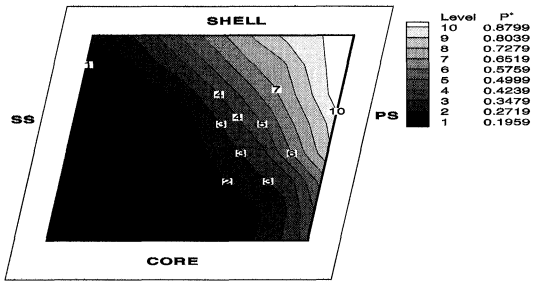

c. Turbine Mid-Chord

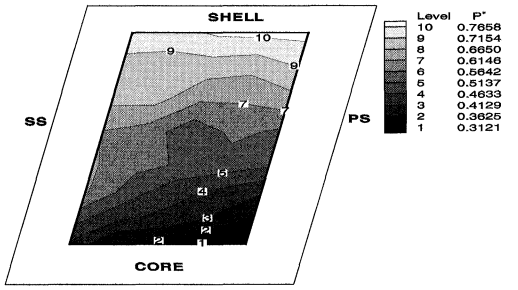

d. Turbine 4/4 Chord

FIGURE 8 Contour plots of rotary stagnation pressure (P^*) ($SR = 0.065$).

exit to the turbine exit at the near stall condition ($SR = 0.065$) are shown in Figure 9. The relative total pressure is significantly higher at the turbine inlet than those observed at other four measurement planes at the near stall condition ($SR = 0.065$). This distribution is pretty similar to the design condition ($SR = 0.6$). The high relative velocity at the pump exit, which contains a high tangentially velocity component, is responsible for this high relative total pressure. The relative total pressure is high near the shell region and low near the core region at all these five measure planes. As explained in Part I, this feature is mainly caused by the "jet-wake" flow structure inside the pump rotor passage, flow separation at the turbine 1/4 chord and mid-chord, and low-mass flow accumulation near the core region. However, the contribution of centrifugal force is negligible, as the rotational speed of turbine at this speed ratio is very small (52 rpm). Thus it can be concluded that the highly non-uniform distribution of relative total pressure is mainly caused by the flow path curvature.

The radial distribution of blade-to-blade averaged turbine torque for the near stall condition ($SR = 0.065$) is shown in Figure 10. The turbine torque is unevenly distributed. Most of the total

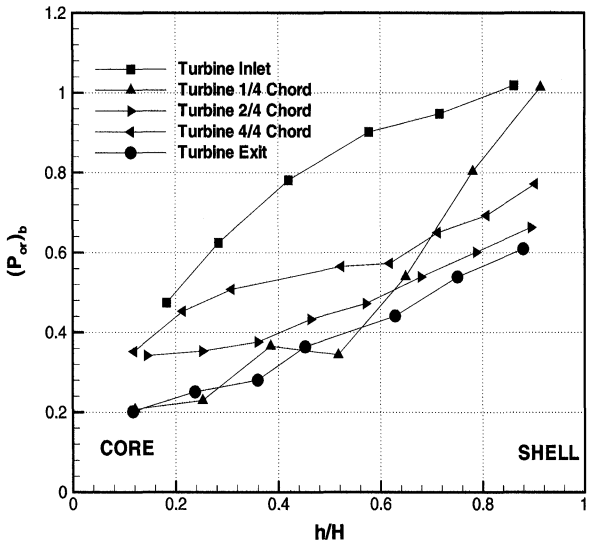

FIGURE 9 Radial distribution of blade-to-blade averaged relative total pressure $(P_{or})_b$ ($SR = 0.065$).

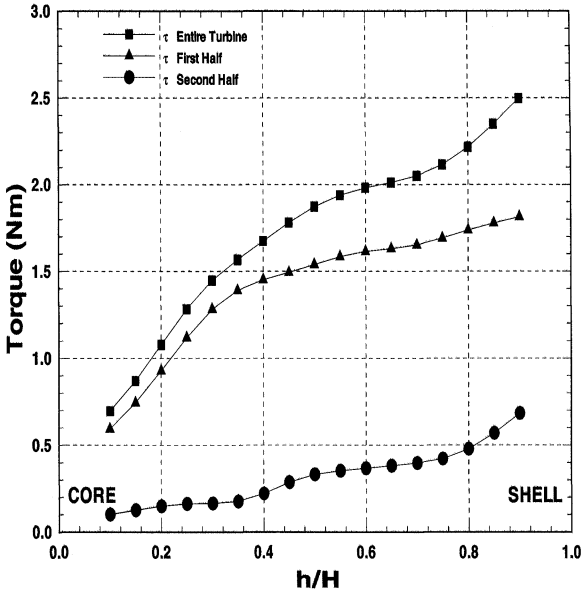

FIGURE 10 Blade-to-blade averaged turbine torque ($SR = 0.065$).

torque (82%) is extracted between the inlet and the middle plane. While for the design condition ($SR = 0.6$), the torque is more evenly distributed with 72% of the total torque extracted between the inlet and the mid-chord plane. The uneven turbine torque distribution at the speed ratio 0.065 is caused by the strong tangential velocity component (preswirl) entering the turbine. Hence, this flow component must be decelerated and redirected by the blades, causing a significant momentum exchanges and torque generation on the blades. The majority of the torque is produced near the shell, which agrees well with the pressure drop data. The shell develops torque at nearly five times the rate of the core. This is due to the higher through flow at the shell, and the larger local blade speeds due to larger radii at the shell. Though there is a much smaller amount of torque created in the second half of the turbine; there is still a modest amount of torque produced near the shell. Since the flow incidence angle does not contribute here, the higher torque production is a result of the higher through flow concentrated near the shell by the centrifugal forces that arise from meridional curvature.

SPEED RATIO EFFECTS ON PRESSURE, INCIDENCE, AND DEVIATION ANGLE

The mass averaged total pressure drop and loss of the turbine at various speed ratios are shown in Figure 11. For centrifugal turbomancinery, significant pressure drop occurs due to the centrifugal force and through the acceleration of relative flow. At high speed ratio, the turbine rotational speed is higher, so is the centrifugal force. This results in higher pressure drop compared to the low speed ratio conditions. Another contribution to the total pressure drop is the flow turning effect. As can be seen from the velocity triangle, the flow turning effect is much more augmented by the blade speed at high speed ratio. At the low speed ratios (such as the near stall condition $SR = 0.065$), the turbine is almost stationary; the only pressure drop source is the viscous loss and the acceleration of the relative flow.

The total pressure loss varies almost linearly with speed ratios. Actually, most of the pressure loss is due to the incidence or shock loss at the turbine leading edge, friction loss along the turbine passage, secondary flow and spanwise mixing losses. The friction loss can be assumed to be proportional to the mean square of the relative flow velocities, and the shock loss can be assumed to be proportional to the square of shock velocity. Because the turbine of the torque converter is designed at speed ratio 0.6 and its peak efficiency condition is speed ratio 0.8. The incidence angle at these two speed ratios is relatively small, and flow separation is not as severe as the near stall condition ($SR = 0.065$). Furthermore, the relative total velocity and the through flow velocity is also higher at the near stall condition ($SR = 0.065$), which may result in higher friction loss. In addition, the non-uniformity in flow parameters is expected to be more severe compared to the design condition and the peak efficiency condition, this may result in extensive mixing losses. Thus, it can be expected that the pressure loss should be higher at the low speed ratios than that at the high speed ratios.

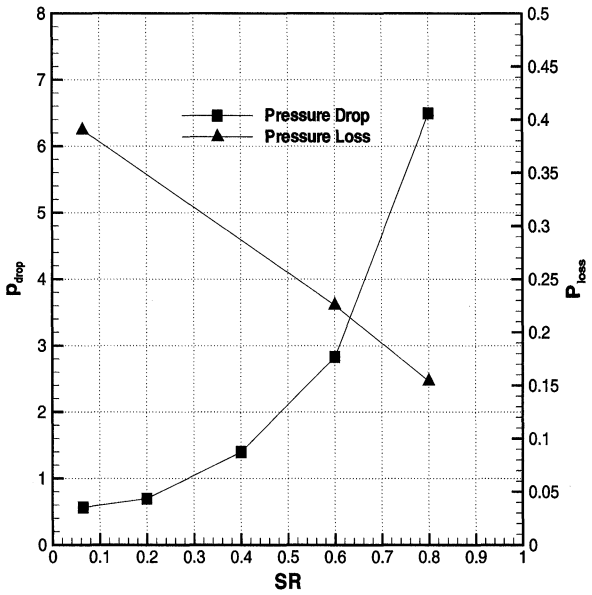

FIGURE 11 Mass averaged total pressure drop, loss *vs.* speed ratio.

The mass averaged incidence near the turbine leading edge and the deviation angle near the turbine trailing edge are shown in Figure 12. The incidence angle is defined as the difference between the inlet flow angle and the physical blade inlet angle. It varies with speed ratios. At speed ratio 0.6, the incidence angle is close to zero. Since the turbine operates at its peak efficiency condition when the incidence angle is negative. At speed ratio 0.8 (the peak efficiency condition), the mass averaged incidence angle is about $-15°$. At other low speed ratios, the incidence angle is positive, and it should be expected that flow separation is likely to happen near the turbine leading edge region due to this positive incidence.

The deviation angle is defined as the difference between the flow angle at the turbine trailing edge and the physical blade outlet angle. It is about 6° at the near stall condition ($SR = 0.065$) and decreases towards the design condition ($SR = 0.6$), which is about 4.5°. At the peak efficiency condition ($SR = 0.8$), the deviation reaches maximum (almost 10°). Since the turbine has 36 blades and the blade passage is long and

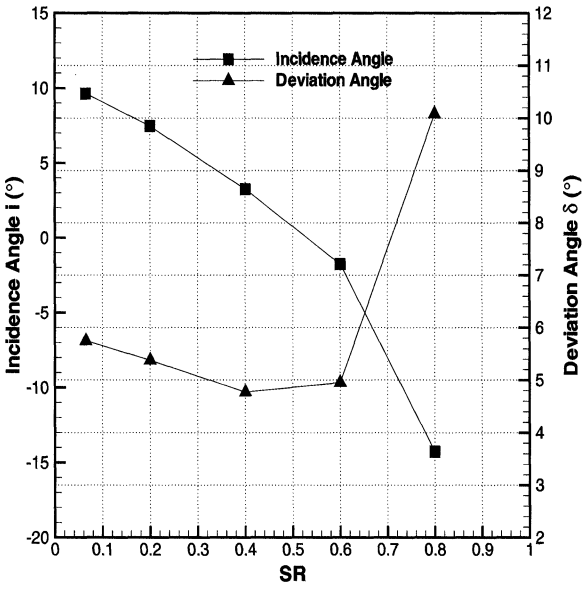

FIGURE 12 Mass averaged incidence, deviation angle *vs.* speed ratio.

narrow, the deviation angle is not likely to be influenced much by the inlet flow angle and the mass flow rate. Thus, the deviation doesn't change much with speed ratios. On the other hand, since there is a jump in deviation angle from speed ratio 0.6 to 0.8, this phenomenon may imply that the incidence effect may play very important role in flow deviation at higher speed ratios.

CONCLUSIONS

Based on the above analysis of the flow field at the near stall condition ($SR = 0.065$) and discussion of the speed ratio effects, the following conclusions can be drawn:

(1) The absolute stagnation pressure drop through the turbine rotor passage is much less at the near stall condition ($SR = 0.065$) than the pressure drop at the design condition ($SR = 0.6$), which can mainly be attributed to the lower rotational speed and the associated lower flow turning effect at this low speed ratio.

(2) The absolute stagnation pressure increases instead of drops from the turbine mid-chord to the turbine 4/4 chord near the core region inside the turbine rotor passage. The large positive incidence angle at the turbine leading edge, the large flow separation area near the core in the first half of the turbine passage, and the flow reattachment before the trailing edge in this region contribute to this phenomenon.

(3) Most of the pressure drop takes place in the first half of the turbine rotor passage, especially in the first quarter at the near stall condition ($SR = 0.065$). This is mainly due to the high incidence angle and the related intense mixing in the large flow separation area near the leading edge at this speed ratio.

(4) The turbine torque at the near stall condition ($SR = 0.065$) is highly uneven distributed, with 84% of the torque generated between the turbine inlet and the middle plane. The uneven torque distribution at this speed ratio is caused by the strong tangential velocity component (preswirl) entering the turbine, causing a significant momentum change in the first half of the turbine rotor passage.

(5) The majority of the torque is produced at the shell at both the design condition ($SR = 0.6$) and the near stall condition ($SR = 0.065$), which is consistent with the pressure drop data. This is due to the higher through flow velocity and the larger local blade speeds at the shell.

(6) The total pressure loss is maximum at the near stall condition ($SR = 0.065$) and varies linearly with the speed ratios. The higher pressure losses at the low speed ratios are attributed to the higher incidence or shock loss near the turbine leading edge, higher friction loss along the turbine passage, and more secondary flow and spanwise mixing loss.

(7) Both the rotation and flow path curvature effects are significant at high speed ratios. At

low speed ratios, however, the dominant factor of the flow field is the centrifugal force due to flow path curvature, that is, both the passage curvature in the meridional plane and the blade curvature on blade-to-blade surface. The Coriolis force due to rotation is insignificant at low speed ratios.

(8) The flow fields between the design condition ($SR = 0.6$) and the off-design conditions have a lot of similarities. However, there also exist significant differences between them. A compromise has to be made between the design and the off-design performance in order to improve the overall performance and fuel economy of torque converters.

Acknowledgments

This project was sponsored by the Powertrain Division of the General Motors Corporation. The authors wish to express their gratitude to Mr. Donald G. Maddock of GM for his assistance, comments, and encouragement. Assistance by Y. Dong is also gratefully acknowledged.

NOMENCLATURE

A	area of passage cross section
h	probe radial height measured from core, mm
H	blade height, mm
h/H	relative radial position ($=0$ at core, $=1$ at shell)
I	incidence angle
n_p	pump rotating speed
n_t	turbine rotating speed
P	static pressure
$(P_0)_a$	absolute stagnation pressure
$(P_{0a})_b$	blade-to-blade averaged absolute stagnation pressure
$(P_{0a})_m$	mass averaged absolute stagnation pressure
$(P_o)_r$	relative total pressure
P^*	rotary stagnation pressure
$P.S$	pressure side
R_o	Rotation number
SR	speed ratio, n_t/n_p
$S.S$	suction side
$(W_o)_t$	relative total velocity
$(W_{ot})_b$	blade-to-blade averaged relative total velocity
W_z	through flow velocity
$(\beta)_t$	relative flow angle
τ	turbine torque
δ	deviation angle

Subscripts

1,2	inlet and exit
r, θ, z	radial, tangential and axial component
b, m	blade-to-blade averaged, mass averaged

References

Burningham, J. (1997) "The Flow Field Through the Turbine of GM 245 mm Torque Converters", *M.S. Thesis*, Department of Aerospace Engineering, The Pennsylvania State University.

Lakshminarayana, B. (1996) "*Fluid Dynamics and Heat Transfer of Turbomachinery*", Wiley-Interscience Publication, John Wiley and Sons, Inc., New York, NY.

Liu, Y. F. and Lakshminarayana, B. (2000) "Flow Field in the Turbine Rotor Passage in an Automotive Torque Converter based on the High Frequency Response Rotating Five-Hole Probe Measurement, Part I: Flow Field at the Design Condition (Speed Ratio 0.6)", *International Journal of Rotating Machinery* (*Submitted*).

Liu, Y. F. (2001) "Experimental and Computational Investigation of Automotive Torque Converter Flow Field", *Ph.D. Thesis*, Department of Aerospace Engineering, The Penn State University.

Marathe, B. V. (1998) "Investigation of 3-D Steady and Unsteady Flow Field Inside an Automotive Torque Converter", *Ph.D. Thesis*, Department of Aerospace Engineering, The Pennsylvania State University.